Plastic deformation of oriented lamellae: 1. Cold rolling of β-phase isotactic polypropylene

T. Asano and Y. Fujiwara
Department of Physics, Faculty of Science, Shizuoka University, Shizuoka, Japan
(Received 12 May 1977)

Isotactic polypropylene was crystallized by the oriented growth method and the oriented β-phase obtained. This has unidirectional lamellar orientation with the lamellar long axis parallel to the growth direction, the lamellae being twisted along this direction. The sample plates were cold-rolled in three orthogonal directions, and the deformation behaviour of each case was investigated chiefly by wide-angle and small-angle X-ray diffraction methods. It was revealed that deformation takes place by a different mechanism in each case, including rotation of lamellae, interlamellar slip, chain-directional and transversal chain slip. These results are discussed in connection with the anisotropic structure of these samples due to the lamellar orientation.

When the β-phase samples are rolled, α-phase crystals appear with *c*-axis orientation and the proportion increases with draw ratio. For crystallographic reasons it is concluded in this case that by stretching the *c*-axis orientation is brought about not through block formation of the original β-phase lamellae and incorporation of these blocks into microfibrils, but by melting or unfolding of the original β-phase lamellae and recrystallization to the *c*-axis-oriented new α-phase.

INTRODUCTION

Various models have been proposed for the deformation mechanism of semicrystalline polymeric substances by drawing, rolling etc.[1–15]. Peterlin *et al.* especially have made precise investigations of the deformation process of polymers, which involves rotation of lamellae, chain tilt and slip, and destruction of lamellae before yielding, and formation of a new structure after yielding.

One fundamental problem, not yet completely answered, about deformation such as drawing is whether the original lamellae are only partly destroyed by deformation and the resultant blocks immediately incorporated in microfibrils at the deformation region, or whether they are completely destroyed and recrystallize again into the same crystal lattice.

The materials hitherto used in investigations are various polymers, especially polyethylene, in the form of unoriented bulk material, two-dimensional spherulites, oriented films (by drawing and annealing), blown films, or single crystals. In these cases there is usually no change in the crystalline structure before and after the deformation. If, however, a sample which never recrystallizes again into the same crystal lattice after destruction can be found, it may be useful to investigate the above problem. The sample used in this work was the β-phase material of isotactic polypropylene which is consistent with the above requirement and has the following properties.

Firstly, when the β-crystals (hexagonal lattice) are destroyed or melt, they do not recrystallize into the same crystalline form but are transformed to the more thermally stable α-crystals (monoclinic lattice), the latter having a melting temperature over 10°C higher. In the α-crystal helical molecules are incorporated as right- and left-handed helices alternately, whereas in the β-crystal all helices are the same[16,17]. Accordingly the phase transition between these crystals needs the rewinding of helices and cannot take place without local unfolding or melting and subsequent recrystallization. This means that when the $\beta \rightarrow \alpha$ phase transition occurs during the deformation, which can be detected easily by the distinct wide-angle X-ray diffraction patterns, it can be concluded that the original β-crystals were destroyed by local melting or unfolding of the lamellae and recrystallized into the α-crystals.

Secondly, this sample has unidirectional lamellar orientation as a result of oriented growth with the lamellar long axis parallel to the growth direction. This is of great advantage in interpreting the X-ray patterns because of the crystallite orientation. Furthermore, with the microbeam X-ray diffraction, a practically single crystal-like pattern can be obtained, which permits the investigation of the detailed deformation process.

Thirdly, the oriented specimen used here corresponds directly to the spherulitic texture as crystallized from the melt, and permits more fundamental investigation than do oriented specimens obtained by drawing and annealing of bulk material often used in the study of lamellar deformation. In the latter specimen, oriented lamellae have developed subsequently as the result of reorganization by annealing, and differ essentially in structure from the crystallized lamellae from the melt. In the case of oriented crystallization, lamellae grow isothermally in the temperature gradient, whereas in the case of usual isothermal melt-crystallization they grow throughout at the same temperature. However, this difference of crystallization condition is considered not to affect essentially the resultant structure of lamellae.

With the sample, which possesses the above characteristics, the deformation mechanism by drawing and by rolling was studied using polarization microscopy, wide-angle and small-angle X-ray diffraction techniques. In this paper, the results of cold rolling are reported.

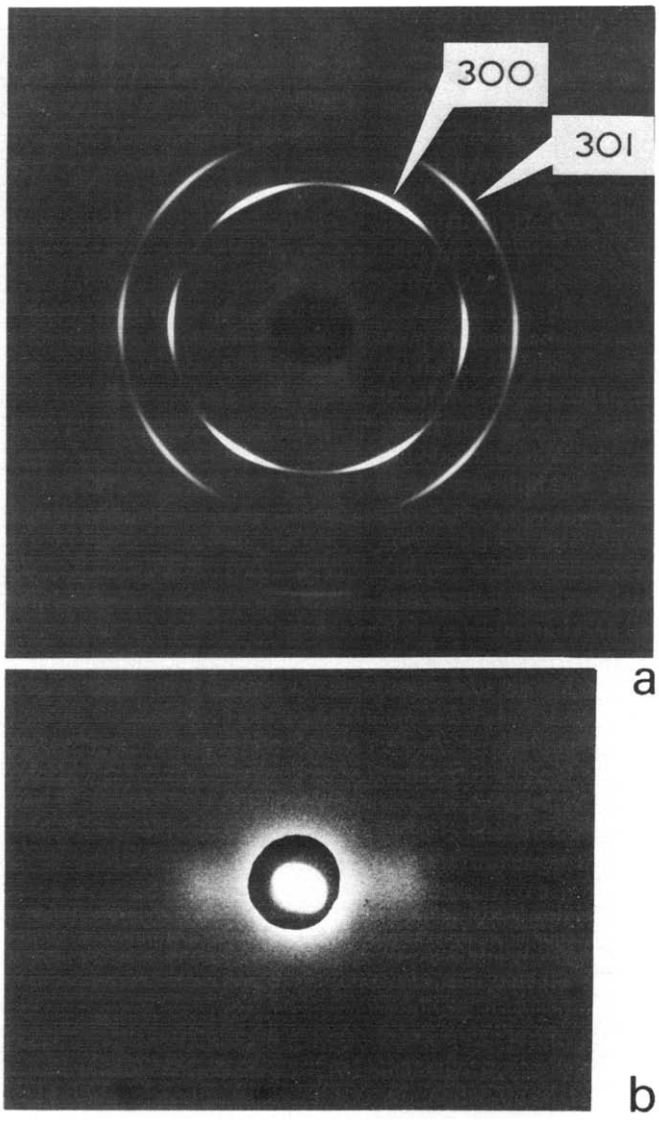

Figure 1 (a) WAXS and (b) SAXS patterns from an oriented β-phase sample. Growth direction vertical. Incident X-ray beam is perpendicular to the film surface

EXPERIMENTAL

Original specimen

The β-phase material was produced by crystallizing the polymer melt in a temperature gradient[18,19]. The main parts of the apparatus for oriented crystallization are a heater whose temperature is controlled to 200°C and a cooler which is placed close to the heater and cooled by water at 20°C. A sample plate, prepared by melt-pressing isotactic polypropylene sheet of 250 μm (in some cases 800 μm) thick between cover glasses, was moved with a suitably chosen constant speed (0.5 ~ 0.7 mm/h in this work) along the temperature gradient between the heater and the cooler, which was about 100°C/mm in the sample plate. The crystallization proceeded steadily at a level in the gradient and effected the production of the spherulitic texture aligned parallel to the moving direction, which corresponds to a radial portion of an ordinary three-dimensional spherulite.

In the case of isotactic polypropylene, the β-phase spherulite (negative spherulite) exceeds the α-phase spherulite (positive spherulite) in the linear growth rate of spherulites. Accordingly, during the oriented crystallization as above, the β-phase spherulite develops preferentially, excluding the α-phase spherulite, and soon occupies the entire available space of the sample plate.

In *Figure 1* the wide-angle X-ray scattering (WAXS) and small-angle X-ray scattering (SAXS) patterns of the oriented β-phase sample are shown. The growth direction in *Figure 1* is vertical. Indices in the WAXS pattern are based on the hexagonal lattice by Samuels *et al.*[17] (a = 19.08 Å, c = 6.49 Å). There are six (300) peaks on the innermost ring and also six (301) peaks outside. A pair of (300) reflections exists on the equator, which indicates that the oriented β-phase crystal is the a-axis orientation. From the SAXS pattern, it is known that the β-phase spherulite is composed of lamellar stacks with the period of 230 Å in 250 μm thick samples and 280 Å in 800 μm thick samples.

A very thin sample with thickness of ~10–20 μm was prepared for microscopic and microbeam X-ray diffraction observation. As is shown in *Figure 2a*, polarization microscope observation reveals the fibrous appearance along the orientation direction composed of 'fibrils' several 10 μm or less in width and also the bright and dark lateral stripes with a period of about 100 μm. The X-ray microdiffraction series was carried out along the growth direction. In *Figure 2b* are shown the microbeam WAXS patterns with incident X-ray perpendicular to the film surface obtained at several positions along the lamellae, and the orientation of unit cell corresponding to *Figure 2b* is also illustrated in *Figure 2c*. This demonstrates that the a-axis is oriented parallel to the growth direction and that the c-axis (molecular axis) perpendicular to it is helically arranged along the a-axis. It was also shown that at the dark stripe molecules are perpendicular and at the bright stripe they are parallel to the sample film, and that the period between neighbouring dark–dark and bright–bright stripes corresponds to a 180° rotation of the c-axis. Accordingly it is known that in the β-phase sample lamellar stacks, where the lamellae are helically arranged along the long axis with a pitch twice the period of stripes (~200 μm) as shown in *Figure 2c*, they are aligned parallel and fairly cooperatively. This circumstance is the same as in the case of polyethylene spherulite[20]. The mechanism of a deformation by rolling was investigated with this sample.

Method of rolling

Cartesian coordinates were defined in the sample film as shown in *Figure 3*, namely, X-axis perpendicular to the film surface, Y-axis parallel to the film surface and perpendicular to the lamellar axis, and Z-axis parallel to the lamellar axis. These axes will be used without change also after the deformation.

Samples were rolled in three ways as follows. A-roll: roll plane parallel to YZ plane and roll direction parallel to Y-axis. B-roll: roll plane parallel to YZ plane and roll direction parallel to Z-axis. C-roll: roll plane parallel to XY plane and roll direction parallel to X-axis. Rolling changes the thickness and length of the sample. By measuring these quantities at each stage of rolling, it was found that thickness varies inversely with change in length. That is, if one denotes the film thickness before and after the rolling as d_0 and d respectively, and the film length before and after as L_0 and L, respectively, and further putting $\tau = d/d_0$ and $\lambda = L/L_0$, it is shown that τ varies almost linearly with $1/\lambda$.

All the rollings were carried out at room temperature. The diameter of the rollers was 5 cm. The sample film was deformed by repeated rolling, gradually narrowing the gap

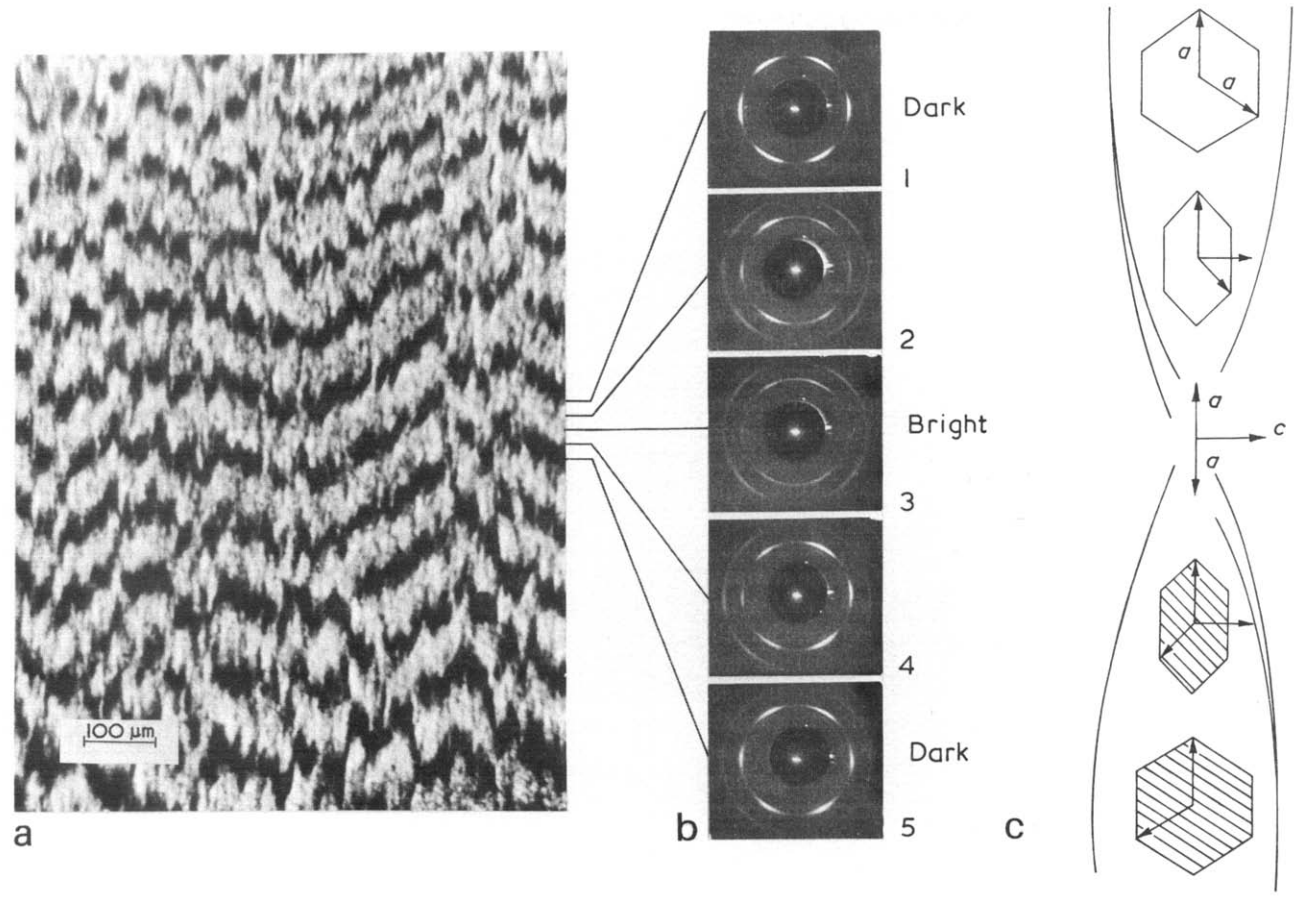

Figure 2 (a) Polarization micrographs of an oriented β-phase sample. The growth direction is vertical and the scale bar represents 100 μm. (b) Microbeam WAXS patterns along the growth direction. The corresponding diffraction positions in the micrographs are connected by lines. (c) Rotation of β-phase unit cells along the growth direction

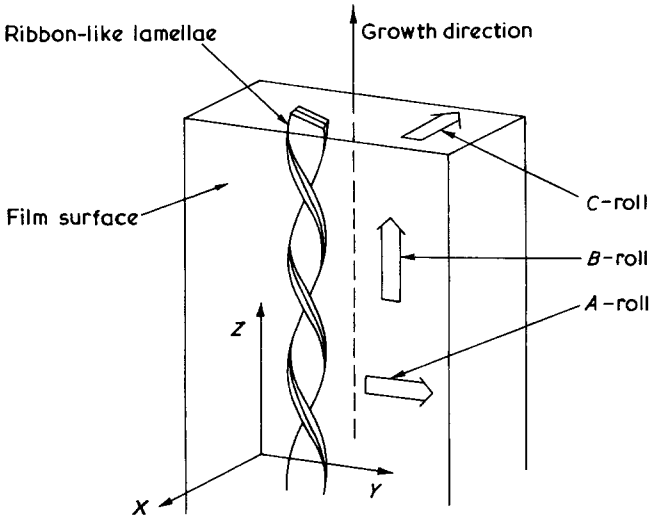

Figure 3 Definition of Cartesian coordinates relative to a sample plate and the definition of three rolling directions

step by step till the intended λ was attained.

The original film thickness was ~250 μm in cases of A- and B-roll, whereas in the case of C-roll strips of ~250 μm in height were cut out parallel to the *XY* plane from the original film of 800 μm thick, and these strips were subjected to rolling.

X-ray diffraction conditions

The X-ray patterns with the incident X-ray beam parallel to *X*-, *Y*-, *and Z*-axes were denoted as *X*-, *Y*-, and *Z*-patterns, respectively. All the X-ray photographs were taken at room temperature in the unclamped state after the rolling. The pinhole diameters of the WAXS and SAXS cameras were 0.2 and 0.3 mm, respectively. The camera distance of the former was 30 mm and that of the latter 360 mm. In the case of microbeam diffraction a 15 μm pinhole slit was used and the camera distance was 7 mm. Rigaku RU3 apparatus was used as the X-ray source with Ni filter for all the diffraction experiments.

RESULTS

A-roll deformation

SAXS measurements were made at each step of the A-roll deformation. Both the *X*- and *Y*-patterns obtained from the original sample (λ = 1) were typical two-point diagrams as shown in *Figure 1b*, while the *Z*-pattern, at λ = 1, was a uniform ring, which represents uniform distribution of lamellae normals around the *Z*-axis. The SAXS *Z*-pattern varied with increasing draw-ratio λ, and the initially uniform diffraction ring split into four separate sections and then changed to a four-point diagram. In the *X*- and *Y*-patterns the two-point diagram disappeared at the initial stage of the deformation and no diffraction maxima except the diffuse scattering around the incident beam were observed above λ = 1.9.

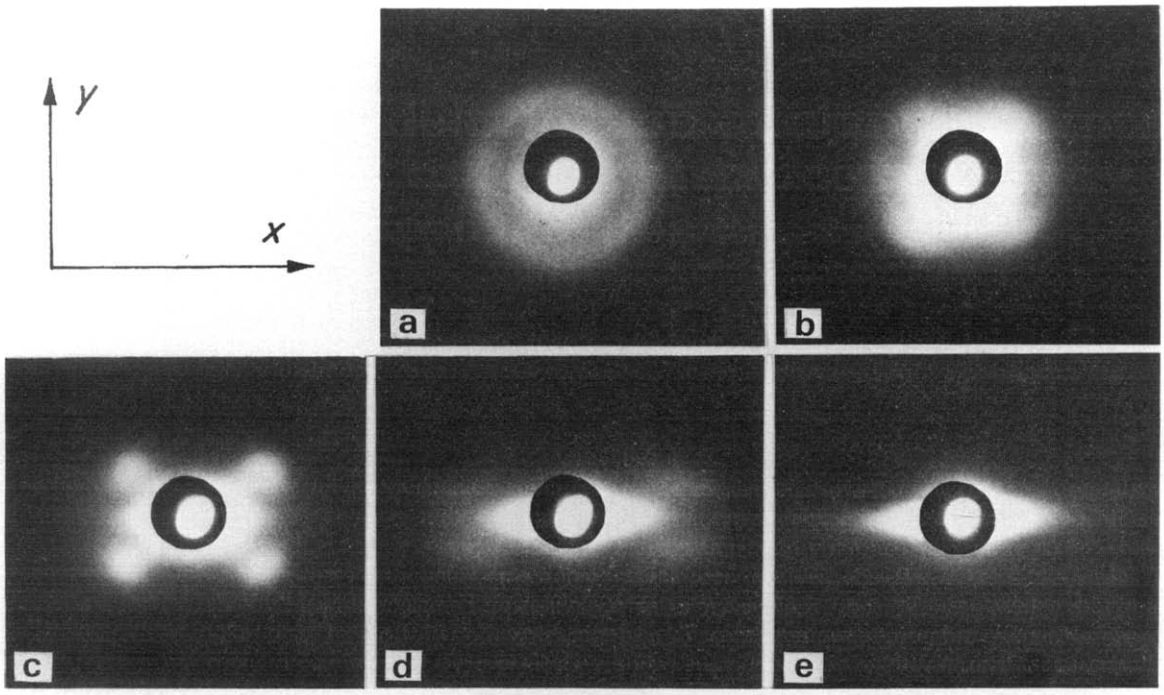

Figure 4 SAXS *Z*-patterns of A-rolled samples at various draw ratios. The roll direction (*Y*-axis) is vertical. (a) λ = 1.0; (b) λ = 1.3; (c) λ = 1.9; (d) λ = 3.2; (e) λ = 5.3

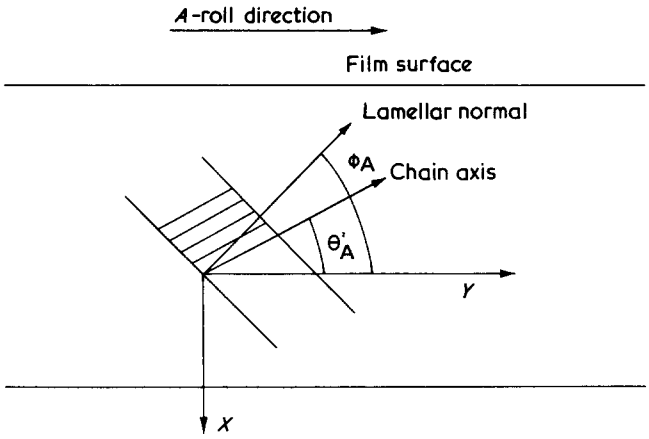

Figure 5 Definition of ϕ_A and θ_A in the A-roll deformation.

Table 1

Draw-ratio, λ	Long spacing, *l* (Å)	ϕ_A (degrees)	θ_A (degrees)	$\phi_A - \theta_A$ (degrees)	Cos $(\phi_A - \theta_A)$	Ratio of long spacing, l/l_0
1.0	230	–	–	–	–	–
1.3	230	45	45	0	1.00	1.00
1.9	220	55	40	15	0.97	0.96
2.5	190	65	30	35	0.82	0.83
3.2	160	75	25	50	0.64	0.70
5.3	–	–	20	–	–	–

A series of SAXS *Z*-patterns during the A-roll deformation is shown in *Figure 4*. In the pattern at λ = 1.3, intensity disappears on the meridian and decreases on the equator, whereas it increases at 45° direction. The spacing obtained from the four-point maxima is still equal to the original one and is 230 Å. A strong scattering is observed around the incident beam. At λ = 1.9, the four-point diagram increases its sharpness and intensity, and is superimposed on an elliptical scattering pattern. The angle between the intensity maximum of the diagonal spots and the *Y*-axis is denoted as ϕ_A which represents the angle between lamellar normal and the *Y*-axis as shown in *Figure 5*. Then, ϕ_A is measured to be 55° which is 10° larger than that at λ = 1.3. The long spacing is reduced to 220 Å. Above λ = 1.9, the scattering around the incident beam shifts to the streak along the equator. At λ = 3.2, the four-point lies on a fairly flat ellipsoid. The long spacing becomes about 160 Å. The values of the long spacing *l* and the angle are given in *Table 1* as a function of λ.

The orientation of the crystalline *c*-axis was observed by WAXS *Z*-pattern. In the original sample, the crystalline *c*-axis is perpendicular to the lamellar surface, i.e., parallel to the lamellar normal. The corresponding WAXS pattern of the original sample shows a uniform (300) ring, which indicates that the *c*-axis is rotated around the *Z*-axis corresponding to the helically twisting ribbon-like lamella. At λ = 1.3, the (300) reflection almost disappears in the meridional and equatorial direction, while the intensity increases at the 45° direction. Here, the angle between the *c*-axis and the roll direction is denoted as θ_A as shown in *Figure 5*. In the initial stage of deformation, θ_A changes in good agreement with ϕ_A, which shows that the *c*-axis is rotated together with the rotation of the lamella. With increasing λ, θ_A decreases whereas ϕ_A increases as shown in *Table 1*. Accordingly the value of $\phi_A - \theta_A$, which indicates the inclination of the crystalline *c*-axis to the lamellar normal, increases with λ. The values of $\phi_A - \theta_A$ are also shown in *Table 1*.

The WAXS *Z*-pattern at λ = 3.2 is shown in *Figure 6*. The (300) reflections have four distinct peaks, from which the angle θ_A is measured to be 25°. There are diffuse scatterings on the equator inside the (300) reflections. They seem to

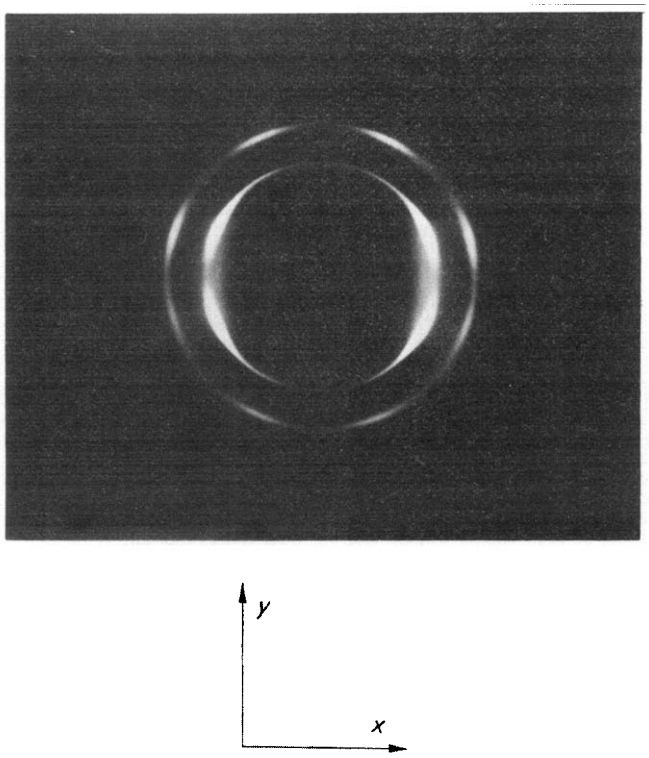

Figure 6 WAXS *Z*-pattern from the sample A-rolled at $\lambda = 3.2$. The roll direction (*Y*-axis) is vertical

originate from imperfect α-phase microcrystallites reported by Peterlin *et al.*[11]. This peak is denoted as α-peak. There is no α-peak in the pattern of the original sample. The α-peak arises during the deformation and its intensity increases with increasing. λ. Therefore, this peak seems to be a reflection from the imperfect α-phase, formed by partial destruction or melting of β-phase lamellae and subsequent rearrangement parallel to the roll direction in the course of the deformation. The intensity of the α-peak is much weaker than that of the β-phase (300) or (301) reflections. It is impossible to discuss the amount of α-phase since the α-peak was so diffuse and indistinct.

The highest draw-ratio obtained in the range of uniform deformation was about five. No further homogeneous deformation was possible, since microcracks arose in the sample. The SAXS pattern at $\lambda = 5.3$ (*Figure 4*) shows a strong streak on the equator and very weak diffuse scattering outside of it near the equator. It is difficult, however, to measure the long spacing because of diffuseness. In the WAXS pattern at $\lambda = 5.3$, the β-phase reflections are still strong, while the α-peak increases its intensity.

In the SAXS and WAXS measurements of the A-roll deformation the *Z*-pattern was mainly observed, the changes in both lamellar and chain orientations occurring mostly in the *XY* plane. It seems that this is related to change in the macroscopic shape of the sample during the A-roll deformation. That is, the starting sample was reduced in thickness in the *X*-direction and stretched in the *Y*-direction, whereas there was no macroscopic change along the *Z*-axis. It seems that plastic deformation of microscopic lamellar structure proceeds in parallel with the deformation of the macroscopic shape.

The SAXS and WAXS patterns at $\lambda = 1.3$ strongly indicate that at the first stage of the deformation lamellae are rotated in the *XY* plane without any reduction in their long spacing or any tilt of the *c*-axis. The fact that the SAXS intensity in the 45° direction increases in the early stage of deformation seems to indicate the existence of a quasistable state of lamellar orientation at this angle. In the case of compressive stress imposed perpendicularly to the sample sheet, the maximum shear stress is imposed on the lamellar surface when the lamella is making an angle 45° to the compression direction. Accordingly, lamellae can easily slip when they are brought to 45° to the surface of the sample and further rotation of the lamellae is prevented by slipping. The lamellar rotation and successive interlamellar slip deformation have previously been reported in the spherulite deformation[7].

With increasing λ, the discrepancy between the angle ϕ_A and θ_A increases as shown in *Table 1*, which indicates that the *c*-axis is tilted within the lamella. This fact suggests that the interlamellar slip and the chain slip along the *c*-axis takes place simultaneously in the deformation. When the *c*-axis is tilted within the lamella, thickness of the crystalline lamella decreases depending on $\cos(\phi_A - \theta_A)$. The values of $\cos(\phi_A - \theta_A)$ are shown in *Table 1* together with the ratios of long spacing to the original one l/l_0. As seen, they coincide with each other fairly well. The long spacing measured from the SAXS pattern represents the average period of the crystalline and amorphous layers. Accordingly, the change in the long spacing includes change in the thickness of the amorphous layer other than that of a crystalline layer. In spite of this fact, however, the good agreement between $\cos(\phi_A - \theta_A)$ and l/l_0 seems to indicate that the change in the long spacing is mainly due to tilt of crystalline *c*-axis within the lamella.

An elliptical four-point diagram has been previously reported by other authors in slightly drawn linear polyethylene and other polymers[8–10]. This is due to the fact that the lamellae parallel to the roll plane are reduced in their spacing by compression, whereas the lamellae perpendicular to the roll direction are increased in their spacing by dilation.

The diffuse scattering around the incident beam seems to be a scattering from voids formed by the deformation. These voids originate by tearing off of lamellae, which is caused by movement of materials during deformation. In the case of slip between lamellae, particularly, the lamellae are partly broken by the tension of taut tie chains and voids are formed in the vicinity when the stress is removed. The central streak observed in the SAXS *Z*-pattern above $\lambda = 1.9$, indicates that the voids have an anisotropic shape. A central streak was also observed in the SAXS *Y*-patterns above $\lambda = 1.9$, while there were no central streaks in the *X*-patterns. Accordingly, the shape of the streak in the reciprocal space is long along the *X*-axis, which indicates that the voids are expanded in the *YZ* plane.

In the observation of a thin film using a polarization microscope, a remarkable change was recognized at the initial stage of the A-roll deformation. The bright and dark stripes seen in the original sample become indistinct and change to all-over uniform brightness at $\lambda = 1.5$. This seems to coincide with the rotation of lamellae observed from the SAXS and WAXS measurements, i.e. as a result of rotation, the crystalline *c*-axes at the bright and dark stripes initially oriented parallel and perpendicular to the sample surface, respectively, are both inclined to about 45°. Thus, the polarization microscope picture changes to uniform appearance since all chains are inclined by the same angle.

The microbeam WAXS was carried out at positions of bright and dark stripes with a thin film A-rolled to $\lambda = 1.5$. The results also indicated that the chains which are oriented originally parallel or perpendicular to the sample surface are

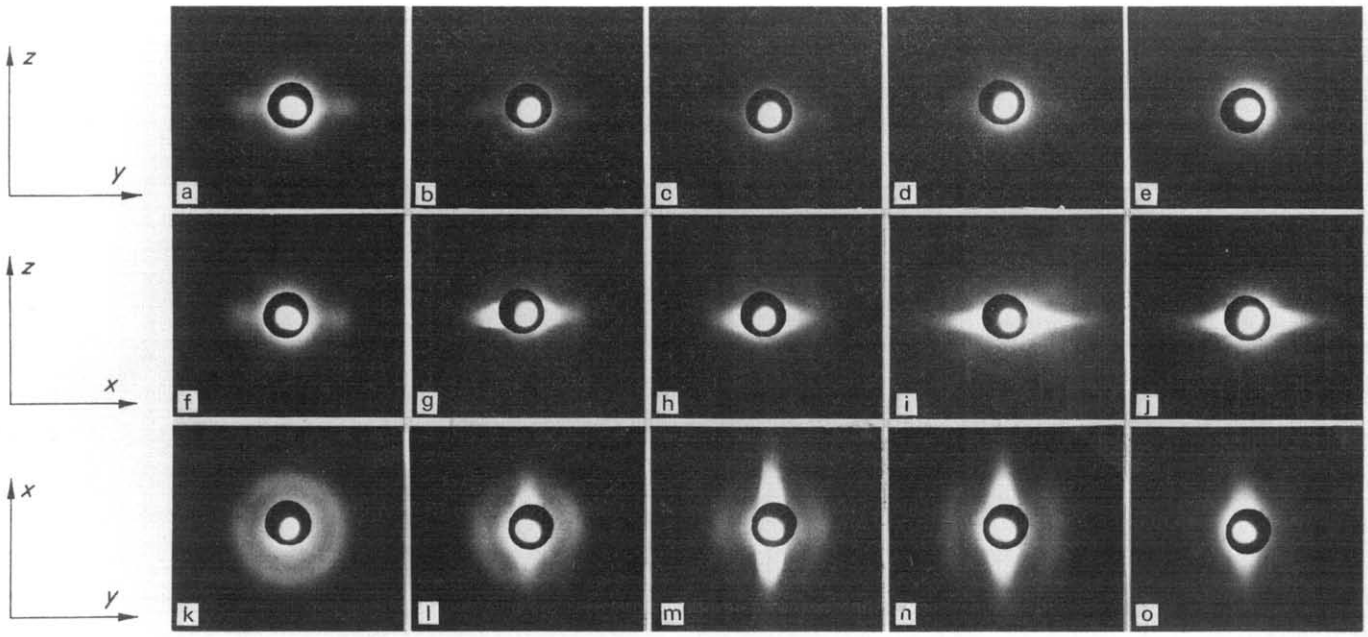

Figure 7 SAXS *X*- [(a)–(e)], *Y*- [(f)–(j)], and *Z*- [(k)–(o)] patterns of B-rolled samples at various draw ratios. (a), (f), (k) $\lambda = 1.0$; (b), (g), (l) $\lambda = 1.3$; (c), (h), (m) $\lambda = 1.9$; (d), (i), (n) $\lambda = 3.3$; (e), (j), (o) $\lambda = 5.8$

rotated about 45°. This fact agrees with the results obtained above.

From these results the deformation mechanisms of A-roll are summarized as follows: at the first stage of deformation rotation of lamellae occurs until almost all the lamellae are inclined about 45° to the roll direction. The following deformation is proceeded by interlamellar slip as observed at $\lambda = 1.3$, and a little later by the slip between crystalline molecules along *c*-axis as observed at $\lambda = 1.9$. As a result of the chain slip, the *c*-axis is tilted in the lamella and the long spacing is decreased with increasing λ. The intensity of the α-peak increases with increasing λ, which shows that the β-phase crystals are partially broken and then imperfect α-phase are formed in the process of the deformation. The WAXS reflections from the β-phase crystals still exist even at $\lambda = 5.3$.

B-roll deformation

The SAXS patterns at several stages of the B-roll deformation are shown in *Figure 7*. In the *Z*-patterns, the original uniform ring begins to disappear in the meridional direction at $\lambda = 1.3$. At $\lambda = 1.9$, the ring remains as arcs spreading over the range about ±45° from the equator. At $\lambda = 3.3$, the reflection seems to lie on an ellipsoid. The long spacing measured from the remaining equatorial reflection does not change with λ.

On the other hand, in the SAXS *Y*-patterns the typical two-point diagram from the original sample gradually changes to longitudinal arcs at $\lambda = 1.3$ and thereafter to a very diffuse four-point diagram at $\lambda = 3.3$. The observed maximum inclination of the lamellae is 20° ~ 30°. The original long spacing of 230 Å reduces to 200 Å at $\lambda = 3.3$. In the *X*-patterns, the typical two-point diagram is preserved and the long spacing does not change with increasing λ until 3.3. At $\lambda = 5.8$, the *X*-, *Y*-, and *Z*-patterns show no diffraction maxima.

The central diffuse scattering or streak also appears in the SAXS *Y*- and *Z*-patterns above $\lambda = 1.3$, where the streaks spread along the *X*-axis in the reciprocal space. This indicates that the shape of the voids is expanded in the *YZ* plane.

Here, one designates the lamella whose normal is parallel to the *Y*-axis in the original sample as *E*-lamella (edge-on lamella) and the lamella whose normal is parallel to the *X*-axis in the original sample as *F*-lamella (flat-lying lamella). In the SAXS measurement, the reflection from the *E*-lamella appears mainly on the *X*-patterns, whereas that from the *F*-lamella does in general on the *Y*-patterns. The inclination of all the lamellae are well shown in the *Z*-patterns. Considering that the crystalline *c*-axis is parallel to the lamellar normal in the original sample, it is known that the WAXS (300) reflections in the *Y*- and *X*-pattern are brought about chiefly from the *E*- and *F*-lamellae, respectively.

The results obtained from the SAXS *X*- and *Y*-pattern indicate that the *E*- and *F*-lamellae show different behaviour during the B-roll deformation; the *E*-lamella remains unchanged both in the orientation and in the spacing, whereas the *F*-lamella inclines some 30° in the *XZ* plane and the spacing decreases to 200 Å at $\lambda = 3.3$. The SAXS *Z*-pattern indicates that the deformational behaviour of the intermediately positioned lamellae is a mixture of both types of deformation depending on their orientation.

The WAXS *X*- and *Y*-patterns at $\lambda = 3.3$ are shown in *Figure 8*. In the *X*-pattern, hexagonal symmetry of the (300) reflection changes to four maxima (one pair are sharp equatorial arcs and another pair are broad meridional arcs), from which it is shown that the *c*-axis is tilted in the *XZ* plane. It is difficult, however, to measure the precise inclination angle (the angle between *c*-axis and *X*-axis) from the SAXS *X*-pattern since it is impossible to observe the distribution of the *c*-axis from one WAXS pattern. For the purpose of measuring this angle, several WAXS patterns were taken varying the direction of the incident beam between the *X*- and *Z*-axis and were examined comparing the intensity and orientation of the (300) reflections. The inclination angle thus obtained was 50° ~ 60° at $\lambda = 3.3$. On the other hand the *Y*-pattern shows no evidence for the tilt of the *c*-axis except the rotation of (300) reflections around the *Y*-axis. This rotation ceases after exactly 30° rotation is attained and no further rotation occurs over $\lambda = 3.3$. The degree of orientation of the (300)

reflection at $\lambda = 3.3$ is found to become sharper in comparison with that of the original sample.

In the case of B-roll deformation, compression stress is imposed perpendicularly to the *YZ* plane and strain occurs mainly in the *XZ* plane. Accordingly, the chain axes of the *E*-lamella crystals are perpendicular to the strain, so that the (300) ⟨1$\bar{2}$0⟩ transverse slip is expected to be favoured, which has been reported in the deformation of polytetrafluoroethylene hexagonal lattice by Young[21]. Because of the hexagonal symmetry of the crystalline form there are three possible (300) transverse slip systems at an angle of 60° to each other, which are perpendicular and ±30° to the compression direction in the original sample. Slip will take place in the (300) plane which experiences the highest resolved shear stress and the crystal rotates until this plane is at 60° to the compression direction. At this angle another plane is also at 60° to the *X*-axis and slip then takes place on both of these planes simultaneously. This is known as the duplex slip and there is no further rotation of the crystal.

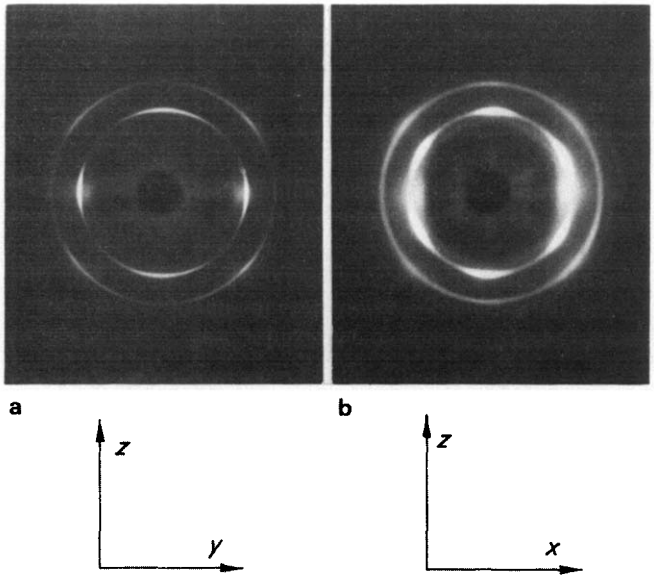

Figure 8 WAXS *X*- and *Y*-patterns of the sample B-rolled at $\lambda =$, 3.3. *Z*-axis is vertical. (a) *X*-pattern: (b) *Y*-pattern

In the WAXS *X*- and *Y*-patterns at $\lambda = 3.3$ (*Figure 8*), diffuse reflections are observed inside the β-phase (300) reflections, the former are the α-peaks as observed in the A-roll deformation. The α-peak appears during the deformation on the equator of WAXS *X*- and *Y*-patterns and its intensity increases with increasing λ. It is considered, like the A-roll, to originate from imperfect α-phase whose *c*-axis is oriented parallel to *Z*-axis.

The results obtained both by the SAXS and WAXS measurements indicate that the mechanism of the B-roll deformation is different for the *E*- and *F*-lamellae and can be summarized as follows: in the *F*- and the neighbouring lamellae, the deformation seems to develop mainly by the chain slip along the chain direction, resulting in the tilting of *c*-axis in the *F*-lamella. In the *E*- and the neighbouring lamellae, the deformation seems to develop by the (300) ⟨120⟩ transverse slip without any inclination of the *c*-axis and the lamellar normal. As the consequence of the duplex slip, the degree of orientation of (300) reflections is increased during the deformation process. In the lamellae between the *E*- and *F*-directions, both of these two deformation mechanisms may operate depending on their orientation.

Observations by the polarization microscope were carried out for the B-rolled thin film. The spacing of the dark and bright stripes was extended by the deformation, but, unlike the case of A-roll, the stripes were visible even at $\lambda = 5.0$. This may be related to the different deformation mechanisms in the dark (*F*-lamellae) and bright (*E*-lamellae) stripes, but the reason is not clear. The microbeam WAXS showed that the orientation of the β-phase molecule is different in the dark and bright stripes, which is consistent with the results obtained by the above experiments, but could not give any new information.

C-roll deformation

In *Figure 9* the SAXS patterns are shown at several stages of λ during C-roll deformation. In the *Z*-patterns, the uni-

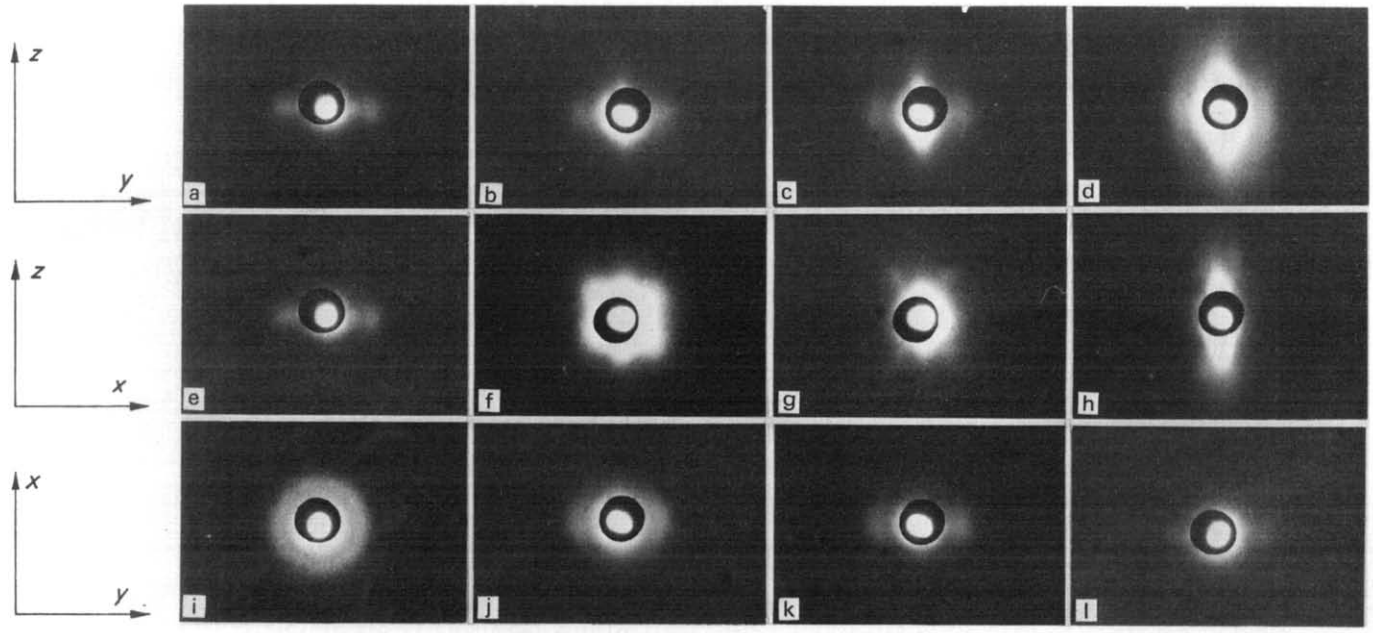

Figure 9 SAXS *X*- [(a)–(d)], *Y*- [(e)–(h)], and *Z*- [(i)–(l)] patterns of C-rolled samples at various draw ratios. (a), (e), (i) $\lambda = 1.0$; (b), (f), (j) $\lambda = 1.3$; (c), (g), (k) $\lambda = 1.9$; (d), (h), (l) $\lambda = 2.8$

Table 2

Draw-ratio, λ	Long spacing, *l* (Å)	ϕ_C (degrees)	θ_C (degrees)	$\phi_C - \theta_C$ (degrees)	Cos $(\phi_C - \theta_C)$	Ratio of long spacing, l/l_0
1.0	280	0	0	0	1.00	1.00
1.3	250	35	~10	~25	~0.91	0.89
1.9	240	50	~20	~30	~0.87	0.86
2.8	220	75	~40	~35	~0.82	0.79

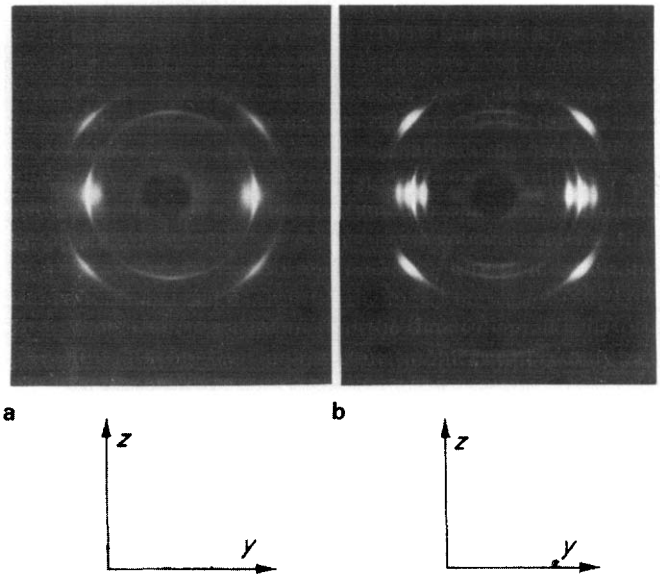

Figure 10 WAXS *X*-patterns of the sample B-rolled at λ = 5.8 (a) before and (b) after annealing treatment at 120°C

form ring at λ = 1 changes to equatorial arcs at λ = 1.3 and to a two-point diagram at λ = 1.9 and 2.8, which indicates that the lamellae normals are inclined from the *XY* plane except the *E*-lamellae. There was no change in the spacing of the *E*-lamellae even at λ = 2.8. On the other hand, in the *Y*-patterns the orientation of the lamellae normal varies largely with λ. The two-point pattern of the original sample changes to the four-point pattern at λ = 1.3. Both the angle of the lamellae normal with respect to the *X*-axis (ϕ_C) and the long spacing (*l*) measured from the *Y*-pattern are changed with increasing λ as shown in *Table 2*. The two-point diagram in the *X*-patterns does not change until λ = 1.9 but then the points extend to arcs along the meridional direction at λ = 2.8. The streaks along the *Z*-axis are observed in the *X*- and *Y*-pattern above λ = 1.3, which indicates that the voids are expanded in the *XY* plane.

The WAXS *Y*-pattern at λ = 2.8 shows that the position of the hexagonally situated (300) reflections is unchanged before and after the deformation but the degree of orientation increases with deformation. This fact indicates that the crystals in the *E*-lamella are deformed by the (300) ⟨1$\bar{2}$0⟩ transverse slip in the same manner as observed in the B-roll deformation, and that alignment of the (300) plane is improved by the duplex slip. In this case, however, the original orientation of three (300) slip planes which are parallel and ±60° to the compression direction, are just suitable for the duplex slip. Accordingly, the *Y*-pattern after deformation does not show any rotation of the (300) reflections. The WAXS *X*-pattern at λ = 2.8 shows that the *c*-axis is rotated in the *XZ* plane. It is difficult, however, to measure the precise inclination angle for the same reason as noted in the WAXS *X*-pattern of the B-rolled sample. This angle (θ_C) was estimated by the same procedure as in the B-roll deformation. The results are shown in *Table 2*.

The results of SAXS and WAXS measurements suggest that the normal of the *F*-lamella is easily rotated in the *XZ* plane at the early stage of the deformation, whereas the rotation of the *c*-axis is relatively small, which means that the *c*-axis is largely tilted in the *F*-lamella and the long spacing is reduced by this tilt in the same manner as was interpreted in the A-roll deformation. In the WAXS *X*- and *Y*-patterns at λ = 2.8, the α-peaks also appear on the equator inside the (300) reflection but their intensity is weaker than that observed in the A- and B-roll deformation.

Summarizing the results in the C-roll deformation, almost all the lamellae except for the *E*-lamellae are inclined with the chain slip along the *c*-axis. Therefore, the lamellae normals are rotated in the *XZ* plane and long spacing decreases by the chain tilt with increasing λ. On the other hand, in the *E*-lamellae, deformation develops by the (300) ⟨1$\bar{2}$0⟩ transverse slip and neither the lamellae normal nor the *c*-axis are inclined during the duplex slip.

Effect of annealing after deformation

The samples stretched by roll deformation were annealed under tension for 2 h at 120°C which is about 30°C lower than the melting temperature of the polypropylene β-phase crystal. The WAXS *X*-patterns of the B-rolled sample before and after the annealing are shown in *Figure 10*. Both the intensity and the sharpness of reflections from the β-phase crystals do not show any change, while those of the α-peak strongly increase by the annealing, which indicates that the perfection of the α-phase crystallites develops on annealing. Other sets of annealing tests were carried out at 120°C for samples varying roll direction and λ. The features of change in WAXS were parallel to the one above.

The SAXS patterns of an A-rolled sample at λ = 5.3 and B-rolled one at λ = 5.8, which were thereafter annealed at 120°C for 2 h are shown in *Figure 11*. New peaks appear on the meridian, whose shape is slightly extended along the layer line. This peak strongly indicates that a new lamellar structure is formed by annealing. The long spacings from both patterns show the same value 170 Å. An A-rolled sample at λ = 3.2 was also annealed at 120°C for 2 h. The change of the α-peaks of the WAXS pattern and the appear-

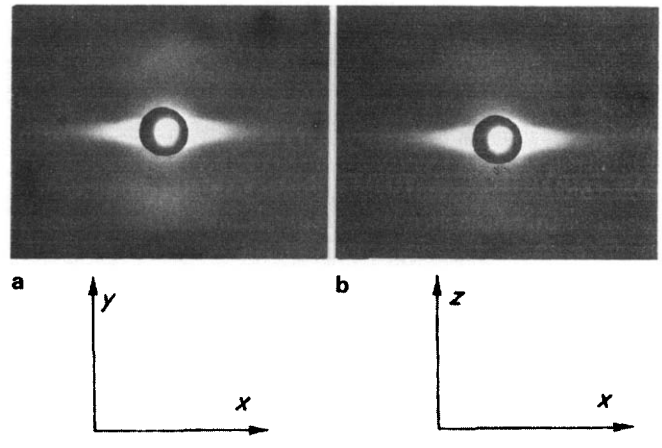

Figure 11 (a) SAXS *Z*-pattern from the sample A-rolled at λ = 5.3 and annealed at 120°C for 2 h. (b) SAXS *Y*-pattern from the sample B-rolled at λ = 5.8 and annealed at 120°C for 2 h

ance of the new peaks in the SAXS pattern occur in the same manner as above. The SAXS peaks are weaker but the long spacing is still about 170 Å.

The similar annealing experiments were carried out at the annealing temperature of 100°C. The changes of the WAXS and SAXS patterns were nearly parallel to those observed at 120°C. However, the long spacing from the new meridional peaks in the SAXS pattern is measured to be about 130 ~ 140 Å.

The characteristics of the SAXS new meridional peaks appearing after the annealing treatment are summarized as follows. (1) The intensity of this peak increases with sharpening of the α-peak in WAXS patterns. (2) The intensity also increases with λ. (3) The long spacing from the peak varies with the annealing temperature. These results indicate that the new meridional peak arises from the new lamellar structure formed by the perfection of α-phase crystallites which are organized by unfolding or partial melting of the β-phase lamellae in the process of the rolling deformation.

DISCUSSION

Anisotropic character of lamellar deformation

The anisotropic behaviour of deformation is likely to depend on the anisotropy of the lamellar structure. The specimen is composed of lamellar stacks grown helically along the orientation axis, and each of these stacks is considered to be a fibrous continuous unit which is very long along the lamellar long axis and probably several 10 μm or less in width as is seen by the microscopic observation. We may conveniently refer to these units as 'fibres'. These fibres are laterally combined with each other by interpenetrating molecules but the degree of combination is considered to be different compared with the continuity along the lamellar long axis. When the fibres are deformed by rolling, the material transportation by deformation is considered to be anisotropic. The stress applied on the specimen by rolling is chiefly by pressure. But during the stretching between the rollers, the specimen and the roller may be in the state of 'sticking' to some extent, and the flow velocity of material in the neighbourhood of the roller surface is equal to the roller velocity, whereas the flow velocity of inside material is different from the roller velocity. This effect is likely to exert some shear stress on the specimen material.

In the case of A-roll, the fibres can readily move with their axes parallel to the *Z*-axis rotating themselves around the fibre axis owing to the shear stress. The rotation of lamellae progresses until 45° orientation to the sample surface is reached where the shear stress between the lamellae composing the fibre become maximal, and then further rotation is suppressed owing to the slipping between the lamellae, leaving them at 45° orientation to the sample surface. Further deformation advances the further interlamellar slipping and as a result the lamellae normal is forced to rotate slowly in the *XY* plane and gradually approaches the *X*-axis. Besides molecular slip along the chain direction is also caused, resulting in the reduction of the lamellar thickness.

In the case of B-roll, the fibres are stretched along the long axis. In this case, the lamellae do not deform with an unifying deformation behaviour, but deform with a different behaviour at each orientation of the lamellae, so as to relax the applied stress most effectively. As the result, transversal slip of molecules is caused in the *E*-lamellae, whereas in the *F*-lamellae chain-directional slip between lamellar molecules is caused. In the latter case, if a large, local chain slip is caused anywhere in a lamellar stack, a dislocation gap is formed, thus dividing the lamellar stacks into many blocks and resulting the lamellar rotation to some extent in consequence.

In the case of C-roll, the roll plane is vertical to the orientation axis of the lamellae. In this case, the material transportation accompanying the deformation exerts an action so as to bend the fibres. Accordingly, the originally vertical lamellae incline strongly accompanying the interlamellar slip, and the molecules in the lamellae tilt strongly by chain-directional slip. However the *E*-lamellae do not show interlamellar slip as no slipping shear stress is applied between these lamellae, but deform by the intralamellar transversal slip.

Transformation from a- *to* c-*axis orientation*

Generally speaking, when bulk material is stretched by drawing or rolling, the molecules in the crystallite align to the stretching direction and finally attain the *c*-axis oriented structure. In our case the starting material is *a*-axis-oriented. Here the method of transformation from *a*- to *c*-axis orientation becomes of interest. It is especially desirable to obtain some information on the process by which the original lamellar structure is transformed to the new lamellar structure composed of *c*-axis oriented molecules. The problem to be solved is whether blocks of the original lamellar structure are directly incorporated into the new lamellar structure, or whether the molecules recrystallize after unfolding or melting of the original structure.

Peterlin *et al.* have observed meridional reflections of SAXS for specimens of λ = 5 in the case of rolling deformation of polyethylene, which originate from a new lamellar structure composed of *c*-axis-oriented molecules[10]. For the rolling deformation of β-phase polypropylene in our case, however, the β-phase did not show perfect *c*-axis-orientation even for a large λ of say 5. Besides, from the SAXS patterns it is shown that the lamellae normal tends to lie in the normal plane to the rolling direction with increasing λ instead of orienting to the rolling direction, and also that no meridional reflections corresponding to the new lamellar structure by Peterlin *et al.* are observed even for a large λ. Following the subsidiarily heavy roll deformation (A- and B-roll) such as λ = 7 ~ 10 no SAXS reflection was found on the meridian. Accordingly, the deformed structure in our case seems to be quite different from the newly built lamellar structure generally seen in polyethylene or in other polymers. On the other hand, the α-phase crystallites, yielded by local unfolding or melting of molecules of β-phase lamellae, as seen from WAXS patterns, show perfect *c*-axis orientation. The α-phase lamellae, formed at 120°C annealing and giving rise to the meridional reflections of SAXS are supposed to be equivalent to the above new lamellae formed by the rolling deformation of polyethylene. Accordingly the transformation from β-phase *a*-axis-oriented structure to the *c*-axis-oriented one must be followed by the phase transformation from β- to α-crystal. As already referred to in the Introduction, this $\beta \rightarrow \alpha$ transformation implies that the β-phase must once be destroyed by unfolding or melting, owing to the difference of molecular conformation between these crystals.

With the above considerations it is concluded that, in the case of roll deformation of β-phase isotactic polypropylene at the room temperature, the transformation from *a*- to *c*-axis orientation takes place not through breaking up of the original lamellae into blocks and incorporating into the new lamellae, but through unfolding or melting and subsequent recrystallization.

ACKNOWLEDGEMENT

The authors are indebted to Professor T. Yoshida of our laboratory for his helpful discussions and advice.

REFERENCES

1 Hay, I. L. and Keller, A. *Kolloid Z. Z. Polym.* 1965, **204**, 43
2 Geil, P. H. 'Polymer Single Crystals', Interscience, New York, 1964, p 445
3 Kiho, H., Peterlin, A. and Geil, P. H. *J. Appl. Phys.* 1964, **35**, 1599
4 Peterlin, A., Ingram, P. and Kiho, H. *Makromol. Chem.* 1965, **86**, 294
5 Kobayashi, K. and Nagasawa, T. *J. Polym. Sci. (C)* 1966, **15**, 163
6 Corneliussen, R. and Peterlin, A. *Makromol. Chem.* 1967, **105**, 193
7 Peterlin, A. *Kolloid Z. Z. Polym.* 1969, **233**, 857
8 Peterlin, A. and Balta-Calleja, F. J. *J. Appl. Phys.* 1969, **40**, 4238
9 Meinel, G., Morosoff, N. and Peterlin, A. *J. Polym. Sci. (A-2)* 1970, **8**, 1723
10 Meinel, G. and Peterlin, A. *Kolloid Z. Z. Polym.* 1970, **242**, 1151
11 Morosoff, N. and Peterlin, A. *J. Polym. Sci. (A-2)* 1972, **10**, 1237
12 Sakaoku, K., Morosoff, N. and Peterlin, A. *J. Polym. Sci. (Polym. Phys. Edn)* 1973, **11**, 31
13 Peterlin, A. *Kolloid Z. Z. Polym.* 1975, **253**, 809
14 Young, R. J., Bowden, P. B., Ritchie, J. M. and Rider, J. G. *J. Mater. Sci.* 1973, **8**, 23
15 Pope, D. P. and Keller, A. *J. Mater. Sci.* 1974, **9**, 920
16 Turner-Jones, A., Aizlewood, Z. M. and Beckett, D. R. *Makromol. Chem.* 1964, **75**, 134
17 Samuels, R. J. and Yee, R. Y. *J. Polym. Sci. (A-2)* 1972, **10**, 385
18 Tanaka, K., Seto, T. and Fujiwara, Y. *Rep. Prog. Polym. Phys. Jpn* 1963, p 285
19 Fujiwara, Y. *Kolloid Z. Z. Polym.* 1968, **226**, 135
20 Fujiwara, Y. *J. Appl. Polym. Sci.* 1960, **4**, 10
21 Young, R. J. *Polymer* 1975, **16**, 450